Impact of contact preference on social contagions on complex networks

Lilei Han,[1] Zhaohua Lin,[1] Ming Tang,[1,2,*] Jie Zhou,[1] Yong Zou,[1] and Shuguang Guan[1,†]
[1]*School of Physics and Electronic Science, East China Normal University, Shanghai 200241, China*
[2]*Shanghai Key Laboratory of Multidimensional Information Processing, East China Normal University, Shanghai 200241, China*

(Received 8 October 2019; revised manuscript received 26 February 2020; accepted 1 April 2020; published 24 April 2020)

Preferential contact process limited by contact capacity remarkably affects the spreading dynamics on complex networks, but the influence of this preferential contact in social contagions has not been fully explored. To this end, we propose a behavior spreading model based on the mechanism of preferential contact. The probability in the model that an adopted individual contacts and tries to transmit the behavioral information to one of his/her neighbors depends on the neighbor's degree. Besides, a preferential exponent determines the tendency to contact with either small-degree or large-degree nodes. We use a dynamic messaging method to describe this complex contagion process and verify that the method is accurate to predict the spreading dynamics by numerical simulations on strongly heterogeneous networks. We find that the preferential contact mechanism leads to a crossover phenomenon in the growth of final adoption size. By reducing the preferential exponent, we observe a change from a continuous growth to an explosive growth and then to a continuous growth with the transmission rate of behavioral information. Moreover, we find that there is an optimal preferential exponent which maximizes the final adoption size at a fixed information transmission rate, and this optimal preferential exponent decreases with the information transmission rate. The used theory can be extended to other types of dynamics, and our findings provide useful and general insights into social contagion processes in the real world.

DOI: 10.1103/PhysRevE.101.042308

I. INTRODUCTION

Spreading dynamics on complex networks constitute an active research area in network science, including virus diffusion on computer networks [1], epidemic and rumor spreading on social networks [2], etc. The documented researches mainly focused on outbreak threshold [3], temporal profile [4], stationary states of systems [5], accurate theoretical prediction frameworks [6], and the effective control strategy [7]. They play significant roles in providing people with the early warning signal and the prevention-control in the real world.

Social contagions, as one of the most important spreading dynamics, have attracted growing attention, incorporating the investigations of dynamics of human behaviors and attitudes [8,9]. Unlike biological contagions (e.g., virus and disease spreading) where each contact triggers a transmission with an independent rate (simple contagion), the rate of nodal infection in social contagions depends strongly on the current or previous neighborhood contacts (complex contagions) [11]. During the contacts, the numerous sources will have a social reinforcement effect on the behavior adoption of an individual, which is usually a strongly nonlinear effect, such as the adoption of a newly expensive drug [10]. When another of his or her friends adopt the behavior, the adoption rate of an individual, surrounded by several friends adopting a particular behavior before a specific time, will be enhanced. There are mounting studies insofar showing that the reinforcement plays an important role in social contagion dynamics [10,12] and one of the classic models to describe the reinforcement is the threshold model [13], which is based on the Markovian process without memory. The crucial nodal infection mechanism is that an individual can only become infected when a certain critical number of exposures has been exceeded. One important result in the model is that the final cascading size grows continuously and then decreases discontinuously with the increase of mean degree. Given that the dynamic processes of classic threshold model is Markovian and the behavior of individual adoption exhibit a memory effect of past exposures, some non-Markovian contagion models have been proposed [10].

The tacit assumption employed in these studies is that an individual can contact all of his or her neighbors in each time step (which is described as reactive process). However, owing to inelastic resources such as limited time and energy, individuals usually have insufficient attention to social interaction and thus have limited contact capacities [14]. In scientific cooperation networks (e.g., conference networks of network science), a scientist can exchange expertise in new fields with only an insufficient fraction of the other scientists in a short time period, leading to the limited diffusion of knowledge [14]. In online social networks (e.g., email communication network), users tend to send the message of a new application (e.g., registration link to Facebook) to their familiar friends rather than the declared strange friends [15]. Researchers have investigated the spreading dynamics with contact process and found that its nontrivial critical behavior can not be quantitatively predicted by mean-field theory [16]. Besides, other studies have explored the effect of contact capacity on epidemic spreading [17] and significantly noted that the

*tangminghan007@gmail.com
†sguan@phy.ecnu.edu.cn

limited contact capacity can enhance the outbreak threshold of epidemics [18]. In social contagions, enlarging the contact capacity can induce a crossover phenomenon of phase transition. The dependence of the final adoption size on the information transmission rate changes from being continuous to being discontinuous [19].

Most previous studies on contact-process model assume that an individual randomly contacts anyone of his or her neighbors with the equal probability. In real world, the contact process is not completely random but preferential. For instance, an individual tends to contact more frequently with his or her emotionally closed friends [20]. Compared with the large-degree nodes usually having weaker ties, the small-degree nodes often have strong ties and thus will be contacted more frequently by their neighboring nodes in mobile phone networks [21]. Yang *et al.* studied the effect of biased contact process on spreading dynamics on uncorrelated networks and the results indicate that the outbreak size can be greatly enhanced if the small-degree nodes are preferentially selected [22]. Considering the degree-correlated networks, Gao *et al.* proposed a preferential contact strategy based on the local network structure and local informed density to promote the information spreading, demonstrating that a moderate correlation coefficient results in the most efficient information spreading [23].

In this paper, we focus on how the preferential contact process influences social contagions. We first propose a behavior spreading model with preferential contacts, where the probability that one adopted node contacts and attempts to transmit the behavioral information to one of his or her neighbor is dependent on the degree of neighbor. The preferential exponent determines the tendency to contact small-degree or large-degree nodes. To quantitatively understand the effects of the preferential contact process on the behavior spreading, we use a dynamic message-passing method. The theoretical predictions from the used method agree well with the numerical simulation results. We find that the increasing preferential exponent will induce a crossover phenomenon of phase transition and the dependence of the final adoption size on the transmission rate of behavioral information changes from the continuous to explosive and then to continuous. The results also demonstrate that the final behavior adoption size first increases and then decreases with the preferential exponent raising, namely existing an optimal exponent to maximize the outbreak size of adoption. The fascinating is that the optimal preferential exponent decreases with the information transmission rate growing, which is distinct from the case in the classic epidemic spreading.

The paper is organized as follows. Section II introduces the behavior spreading model with preferential contacts. The dynamic message-passing method is described in Sec. III. Section IV shows the numerical simulation results and its theoretical ones. Section V ends up with a conclusion and discussion.

II. BEHAVIOR SPREADING MODEL IN THE PREFERENTIAL CONTACT PROCESS

The uncorrelated configuration network model is used to generate uncorrelated heterogeneous networks under a given degree distribution $P(k)$ [2]. On the heterogeneous networks, we use a generalized stochastic susceptible-adopted-recovered (SAR) model to describe social contagions such as behavior spreading [24]. At each time step, each node can be in one of the three different states: susceptible state, adopted state, and recovered state. In the susceptible state, a node does not adopt the behavior. In the adopted state, a node adopts the behavior and tries to transmit the behavioral information to his or her selected neighbors. In the recovered state, a node loses interest in the behavior and will not transmit the information further.

To initiate a social contagion, a fraction of A_0 nodes are randomly chosen to be in the adopted state (i.e., seeds) while the other nodes are in the susceptible state. At the beginning of contagion process, all susceptible nodes do not know any information about this behavior and thus the cumulative pieces of information is zero for all of the susceptible nodes. Each susceptible node holds a static adoption threshold κ which reflects his or her interest in adopting the behavior. In simulations, the synchronous updating method is implemented to update the states of nodes [25]. At each time step (e.g., $\Delta t = 1$), each adopted node i with k_i neighbors selects c neighbors according to the preferential contact strategy and tries to transmit the behavioral information to each of the selected neighbors j. In general, we set $c \leqslant k_i$. According to the preferential contact strategy, the probability ω_{ji} that an adopted node i contact one of its neighbors j is given by

$$\omega_{ji} = \frac{k_j^\alpha}{\sum_{l \in \mathcal{N}_i} k_l^\alpha}, \tag{1}$$

where $\mathcal{N}_i$ is the set of neighbors of node i, k_j is the degree of neighbor j, and α is the preferential exponent. The preferential exponent α determines the tendency for a node to contact his or her small-degree or large-degree neighbors. When $\alpha > 0$, large-degree neighbors are preferentially contacted while small-degree neighbors are favored when $\alpha < 0$. When $\alpha = 0$, all neighbors are randomly chosen, which returns to the classical contact process [26]. Considering the contact capacity c, node j will be selected for contacting by node i with probability $c\omega_{ji}$.

If the neighbor j of node i is selected for contacting when he or she is in the susceptible state, node j will receive the information with probability λ; otherwise, nothing happens. Once node i transmits the information to node j successfully, the cumulative pieces of information m that node j ever received will increase by 1. It is noted that the information can not be transmitted between i and j once again in the following contagion process, which means that the redundant information transmission on the edge is forbidden [24]. If the cumulative information m is greater than or equal to the adoption threshold κ, then node j will become adopted in the next time step. At the same time, each adopted node loses interest in the behavior and enters into the recovered state with probability γ. The recovered nodes do not take part in the contagion process. The contagion dynamics terminates once all the adopted nodes become recovered. The behavior spreading is a complex contagion process with social reinforcement effect when $\kappa > 1$. When $\kappa = 1$, it comes back to the classical simple disease spreading.

III. DYNAMIC MESSAGE-PASSING METHOD

In the behavior spreading model with preferential contact, both the social reinforcement effect based on threshold model and the preferential contact strategy based on neighbors' degrees can bring strong dynamical correlations between every pair of connected nodes into the spreading processes. We here use a dynamic message-passing method [27] to describe the behavior spreading in the preferential contact process. We define $\theta_{i\leftarrow j}(t)$ as the probability that a node j has not transmitted the behavioral information to node i by the time t. Assuming that node i is in the cavity state, he/she can not transmit the information to his or her neighbors but can receive the information from his or her neighbors. And the probability that node i receives m cumulative pieces of information by time t is thus given by

$$\phi_i(m,t) = (1-A_0)\left[\sum_{|\Theta|=m}^{\Theta\subseteq\mathcal{N}_i}\prod_{j\in\Theta}(1-\theta_{i\leftarrow j}(t))\prod_{l\in\mathcal{N}_i\setminus\Theta}\theta_{i\leftarrow l}(t)\right]. \tag{2}$$

Here, $\mathcal{N}_i$ is the set of node i's neighbors, and Θ ranges over all subsets of size m in $\mathcal{N}_i$. The formula $1-A_0$ represents that only the nodes initially being in the susceptible state can receive the information from his or her neighbors.

From the description of contagion model, if the received cumulative pieces of information for node i is less than the threshold κ, he or she will still be susceptible at time t. And the probability of node i being in the susceptible state by time t is thus

$$s_i(t) = \sum_{m=0}^{\kappa-1}\phi_i(m,t). \tag{3}$$

Considering all nodes in a network, we can get the density of susceptible nodes at time t as

$$S(t) = \frac{\sum_i s_i(t)}{N}, \tag{4}$$

where N is the size of this network. Similarly, we can get the density of nodes who have received m pieces of information at time t as

$$\Phi(m,t) = \frac{\sum_i \phi_i(m,t)}{N}. \tag{5}$$

According to the definition of $\theta_{i\leftarrow j}(t)$, it can be divided into three cases:

$$\theta_{i\leftarrow j}(t) = \xi^S_{i\leftarrow j}(t) + \xi^A_{i\leftarrow j}(t) + \xi^R_{i\leftarrow j}(t), \tag{6}$$

where $\xi^S_{i\leftarrow j}(t)$, $\xi^A_{i\leftarrow j}(t)$ and $\xi^R_{i\leftarrow j}(t)$, respectively, represent the probabilities that node j is in the susceptible, adopted, and recovered states and has not transmitted the information to the neighboring node i by time t.

If node j is susceptible initially, he or she cannot receive the information from node i since node i is in the cavity state. But he or she can receive information from the other neighbors. Similar to Eq. (2), the probability that node j receives m cumulative pieces of information by time t is given by

$$\phi_{j\setminus i}(m,t) = (1-A_0)\left\{\sum_{|\Theta|=m}^{\Theta\subseteq\mathcal{N}_j\setminus i}\prod_{l\in\Theta}[1-\theta_{j\leftarrow l}(t)]\prod_{l\in\mathcal{N}_j\setminus\{\Theta,i\}}\theta_{j\leftarrow l}(t)\right\}. \tag{7}$$

And then we can get the probability that node j is susceptible and has not transmitted the information to node i as

$$\xi^S_{i\leftarrow j}(t) = \sum_{m=0}^{\kappa-1}\phi_{j\setminus i}(m,t). \tag{8}$$

Once node j transmits the information via the edge $i\leftarrow j$, $\theta_{i\leftarrow j}$ will decrease. In this case, there are two basic processes. (a) Node j contacts node i via the edge with rate $c\omega_{ij}$ as shown in Eq. (1). (b) The information is transmitted through the edge with the information transmission rate λ. Therefore, the evolution of $\theta_{i\leftarrow j}(t)$ is given by

$$\frac{d\theta_{i\leftarrow j}(t)}{dt} = -\lambda c\omega_{ij}\xi^A_{i\leftarrow j}(t). \tag{9}$$

If the adopted node j enters into the recovered state with recovery rate γ and meanwhile has not transmitted the information to node i, then $\xi^R_{i\leftarrow j}(t)$ will increase. Thus, we have

$$\frac{d\xi^R_{i\leftarrow j}(t)}{dt} = \gamma(1-\lambda c\omega_{ij})\xi^A_{i\leftarrow j}(t). \tag{10}$$

Combining Eqs. (9) and (10) and the initial situations [i.e., $\theta_{i\leftarrow j}(0)=1$ and $\xi^R_{i\leftarrow j}(0)=0$], we can get the expression of $\xi^R_{i\leftarrow j}(t)$ as

$$\xi^R_{i\leftarrow j}(t) = \gamma\left(\frac{1}{\lambda c\omega_{ij}}-1\right)[1-\theta_{i\leftarrow j}(t)]. \tag{11}$$

Substituting Eqs. (6), (8), and (11) into Eq. (9), we can obtain the time evolution of $\theta_{i\leftarrow j}(t)$ as

$$\frac{d\theta_{i\leftarrow j}(t)}{dt} = \lambda c\omega_{ij}\left[\sum_{m=0}^{\kappa-1}\phi_{j\setminus i}(m,t)-\theta_{i\leftarrow j}(t)\right] + \gamma[1-\theta_{i\leftarrow j}(t)](1-\lambda c\omega_{ij}). \tag{12}$$

We denote $S(t)$, $A(t)$, and $R(t)$ as the densities of susceptible, adopted, and recovered nodes at time t, respectively. According to the model description in Sec. II, we can write the evolution equations of the adopted density and the recovered density as

$$\frac{dA(t)}{dt} = -\frac{dS(t)}{dt} - \gamma A(t) \tag{13}$$

and

$$\frac{dR(t)}{dt} = \gamma A(t), \tag{14}$$

respectively. From the above, we know that Eqs. (2)–(4), (7), and (12)–(14) provide a complete and general description of the social contagions based on preferential contact.

We are interested in the steady state of the social contagion dynamics when time $t \to \infty$. Setting the right side of Eq. (12) to be zero, we have

$$\theta_{i\leftarrow j}(\infty) = \sum_{m=0}^{\kappa-1} \phi_{j\backslash i}(m,\infty) + \gamma[1-\theta_{i\leftarrow j}(\infty)]\left(\frac{1}{\lambda c \omega_{ij}} - 1\right). \tag{15}$$

We numerically iterate Eqs. (7) and (15) to obtain the value of $\theta_{i\leftarrow j}(\infty)$. Then, we can compute $S(\infty)$ and $R(\infty) = 1 - S(\infty)$ using Eqs. (2)–(4).

When $\kappa = 1$, the contagion process comes back to the classical simple disease spreading. For initial infected density $A_0 \to 0$, a phase transition from negligibly small, vanishing relative epidemic size $R(\infty) = 0$ to an outbreak of a finite relative size $R(\infty) > 0$ occurs with the increase of information transmission rate λ in thermodynamic limit. Due to the nonlinearity of Eqs. (7) and (15), they do not have a closed analytic form and thus we cannot get the analytic expression of the epidemic threshold λ_c. A simple fact is that when $\lambda \to \lambda_c$, the conditions $R(\infty) \to 0$ and $\theta_{j\leftarrow i} \to 1$ satisfy. We define $q_{j\leftarrow i} = 1 - \theta_{j\leftarrow i}$, and then Eq. (7) can be linearized using $q_{j\leftarrow i} \simeq 0$ to become

$$\phi_{j\backslash i} \simeq 1 - \sum M_{i\leftarrow j,h\leftarrow l} q_{h\leftarrow l}. \tag{16}$$

Here $\mathbf{M}$ is the nonbacktracking matrix [28] of the network and

$$M_{i\leftarrow j,h\leftarrow l} = \delta_{jh}(1-\delta_{il}), \tag{17}$$

where δ_{il} is a Dirac δ function. Inserting Eq. (16) into Eq. (15) and neglecting higher-order terms, we have

$$\sum \{\lambda c \omega_{ij}[M_{i\leftarrow j,h\leftarrow l} + (\gamma-1)\delta_{ih}\delta_{lj}] - \delta_{ih}\delta_{lj}\gamma\} q_{h\leftarrow l} = 0. \tag{18}$$

To solve Eq. (18), we define a matrix $\mathbf{J}$ whose elements are

$$J_{i\leftarrow j,h\leftarrow l} = c\omega_{ij}[M_{i\leftarrow j,h\leftarrow l} + (\gamma-1)\delta_{ih}\delta_{lj}]. \tag{19}$$

The system enters a global epidemic region in which the epidemic grows exponentially when the largest eigenvalue of $\mathbf{J}$ is greater than zero [29]. That is, the outbreak size grows exponentially with time. Thus, we can obtain the epidemic threshold as

$$\lambda_c = \frac{\gamma}{\Lambda_J}. \tag{20}$$

When $\kappa > 1$, the behavior spreading is a complex contagion process with social reinforcement effect. A vanishingly small seeds $A_0 \to 0$ can not trigger the global behavior adoption, so the outbreak threshold λ_c is nonexistent.

IV. SIMULATION RESULTS

In this section, we study the impacts of preferential contact process on social contagions on complex networks through extensive simulations. A large number of real-world networks have a highly skewed degree distribution, such as the World Wide Web [30] and Facebook [31]. In simulations, we use the uncorrelated configuration model (UCM) [32] to generate synthetic networks. The degree distribution follows $P(k) \sim k^{-\nu}$, where ν is power-law exponent. We set network size and the minimum degree to be $N = 10^4$ and $k_{\min} = 4$, respectively.

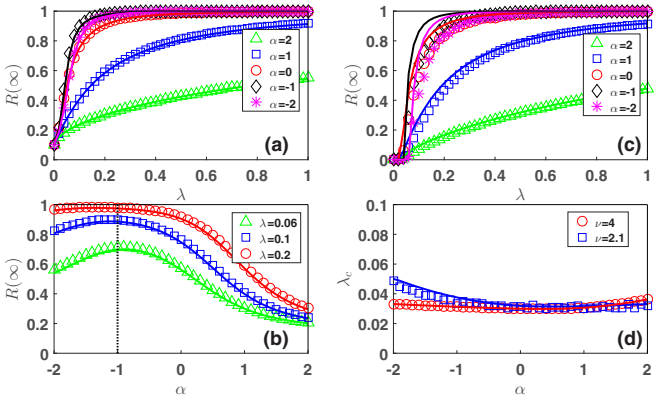

FIG. 1. Effects of preferential contacts on simple contagions. (a) The final adoption size $R(\infty)$ versus the information transmission rate λ for different preferential exponents α when $A_0 = 0.1$, where green up triangles, blue squares, red circles, black diamonds, and mauve asterisks represent the simulation results for $\alpha = 2, 1, 0, -1, -2$, respectively. (b) $R(\infty)$ versus α for different λ values when $A_0 = 0.1$, where red circles, blue squares, and green up triangles represent the simulation results for $\lambda = 0.2, 0.1, 0.06$, respectively. (c) $R(\infty)$ versus λ for different α when $A_0 = 0.0001$. (d) The epidemic threshold λ_c versus α when $A_0 = 0.0001$ which is different from $A_0 = 0.1$ in panels (a) and (b), where the red circles and blue squares represent the numerical thresholds identified by the variability measure for $\nu = 4.0, 2.1$. In panels (a), (b), and (c), the curves are the theoretical predictions from Eqs. (2)–(4), (7), and (15). In panel (d), the curve is the theoretical prediction from Eq. (20). Other parameters are $\nu = 2.1$, $c = 4$, $\kappa = 1$, and $\gamma = 0.1$.

The maximum degree is set to be $k_{\max} \sim \sqrt{N}$ following structural cutoff [33]. Without loss of generality, the limited contact capacity for all nodes is uniformly set to be less than or equal to the minimum degree $k_{\min}$. Here we set the limited contact capacity as $c = 4$. Other parameters are the time interval of each time step $\Delta t = 1$, the recovery rate $\gamma = 0.1$, and the initially adopted density $A_0 = 0.1$. The simulation results in synchronous updating method will approach to that in asynchronous updating method when the recovery rate is smaller than 0.1 [34]. To make sure a complex contagion with social reinforcement effect has a possibility to break out, A_0 is set as a large value. There is thus no phase transition from negligibly small adoption size to an outbreak of a finite relative size. At least 2×10^3 independent dynamical realizations on a fixed network are implemented to calculate the pertinent average values.

We first investigate the effects of the preferential exponent α on the final behavior adoption size $R(\infty)$ for the simple contagion with adoption threshold $\kappa = 1$. From Fig. 1, we see that the theoretical predictions agree well with the simulation results, which verifies the accuracy of the dynamic message-passing method. For any value of α, $R(\infty)$ continuously increases with the increase of λ due to the lack of social reinforcement effect [see Fig. 1(a)]. Another question that we are interested in is how $R(\infty)$ varies with the increase of preference parameter α at a fixed λ. As shown in Fig. 1(b), $R(\infty)$ first increases and then decreases with the increase of α. There is a maximum value of $R(\infty)$ at $\alpha \approx -1$ for any λ

value, which has been testified by Ref. [22]. Heterogeneous networks usually have several hub nodes of large degrees and a large number of nodes with small degrees. A positive (negative) α makes hub (small-degree) nodes be contacted more frequently. Once one contact leads to the transmission of the behavioral information through an edge of a node, all the subsequent contacts on all his or her edges will be invalid due to this node being in the adopted state. Many useless contacts on edges will reduce the outbreak size. A moderate value of $\alpha = -1$ can make almost all of the nodes to be contacted evenly (or infected with the same probability) by their neighbors, which results in a maximum value of $R(\infty)$. Furthermore, we investigate the impact of the preferential exponent α on the epidemic threshold λ_c when $A_0 = 0.0001$ in Fig. 1(d), which is different from $A_0 = 0.1$ in Figs. 1(a) and 1(b). From Fig. 1(d), we see that λ_c first decreases and then increases with the increase of α. A minimum value of λ_c occurs at a positive value of α, which means that preferentially contacting large-degree nodes promotes the outbreak of epidemics.

Next, we investigate the effects of preferential exponent α on the final behavior adoption size $R(\infty)$ for the complex social contagions, e.g., the results for $\kappa = 3$ in Fig. 2. In accordance with the case of simple contagions, the dynamic message-passing method can accurately describe the social contagion dynamics. From Fig. 2(a), we find that the dependence of $R(\infty)$ on λ changes from a continuous growth to a explosive growth and then to a continuous growth with the decrease of α. This crossover phenomenon of growth type can be explained by discussing the changes in the fraction of nodes in the subcritical state from an intuitive perspective. A node in the subcritical state means that he or she is in the susceptible state and the number of cumulative pieces of information is just one smaller than his or her adoption threshold κ [24]. When $\alpha = -2$ or $\alpha = 1$, the final fraction of nodes in the subcritical state $\Phi(\kappa - 1, \infty)$ increases gradually with the increase of λ and thus a continuous growth of $R(\infty)$ with the increase of λ occurs. When $\alpha = -1$, $\Phi(\kappa - 1, \infty)$ first increases with the increase of λ and reaches a maximum at λ_c [see Fig. 2(b)]. Almost all of the subcritical nodes are contacted evenly in this case. A slight increment of λ will induce a finite fraction of $\Phi(\kappa - 1, \infty)$ to adopt the behavior simultaneously (i.e., cascading process). An explosive growth in $R(\infty)$ occurs.

We also investigate the variation of $R(\infty)$ with α when λ is fixed in Fig. 2(c). Similar to the case of simple contagions, $R(\infty)$ first increases and then decreases with the increase of α. There is an extreme point (α_o, R_o). It should be noted that $R(\infty)$ first increases explosively and then decreases continuously when $\lambda = 0.48$. The reason for the explosive growth is consistent with the explosive growth of $R(\infty)$ with the increase of λ. What is more noteworthy is that the optimal value α_o corresponding to the extreme point decreases with the increase of λ. When λ is small, $\alpha_o > 0$ means that preferentially contacting hub nodes with large degrees helps to promote the behavior spreading. When λ is large, $\alpha_o < 0$ means that preferentially contacting small-degree nodes plays an important role in enhancing the behavior spreading. For complex social contagions with social reinforcement effect, the susceptible nodes need to accumulate multiple successful

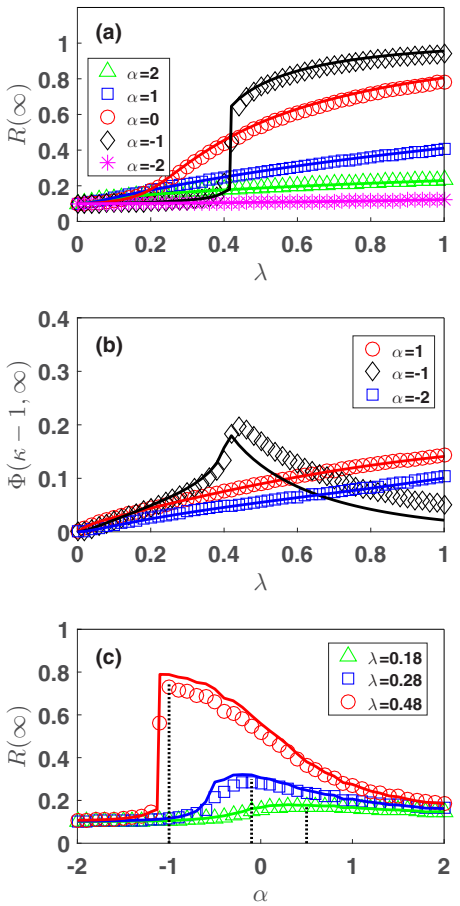

FIG. 2. Effects of preferential contacts on complex contagions. (a) $R(\infty)$ as a function of λ for different values of α, where green up triangles, blue squares, red circles, black diamonds, and mauve asterisks represent the simulation results for $\alpha = 2, 1, 0, -1, -2$, respectively. (b) The final density of subcritical state $\Phi(\kappa - 1, \infty)$ as a function of λ for different values of α, where red circles and black squares are the simulation results for $\alpha = 1, -1$, respectively. (c) $R(\infty)$ as a function of α for different λ values, where red circles, blue squares, and green up triangles represent the simulation results for $\lambda = 0.48, 0.28, 0.18$, respectively. In all panels, the curves are the theoretical predictions from Eqs. (2)–(4), (7), and (15). Other parameters are $\nu = 2.1$, $c = 4$, $\kappa = 3$, and $\gamma = 0.1$.

contacts to reach their own adoption thresholds. When λ is small, the number of contacts that successfully transmit the behavioral information is very small. To enlarge the outbreak size, the adopted nodes should contact as much as possible with a certain part of network nodes. An appropriate value of $\alpha > 0$ makes some hub nodes be contacted frequently and easier to meet the threshold condition, which makes for the behavior spreading. A negative α makes the limited contacts be dispersed over a large number of small-degree nodes and these nodes difficult to reach their threshold conditions, which restrains the behavior spreading. When λ is large, an adopted node can transmit multiple behavioral information successfully through contacts to his or her neighbors. To maximize the final adoption size $R(\infty)$, the contacts that successfully transmit the information need to be scattered on more nodes

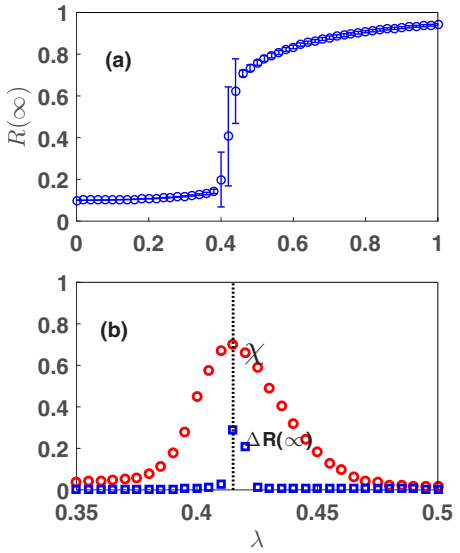

FIG. 3. Comparison of theoretical critical points with numerical critical points of complex contagions on a scale-free network. (a) The final adoption size $R(\infty)$ with error bar as a function of information transmission rate λ. (b) The variability χ (red circles) and the jump size $\Delta R(\lambda, \infty)$ (blue squares) versus λ. Other parameters are $\nu = 2.1$, $c = 4$, $\kappa = 3$, $\gamma = 0.1$, and $\alpha = -1$.

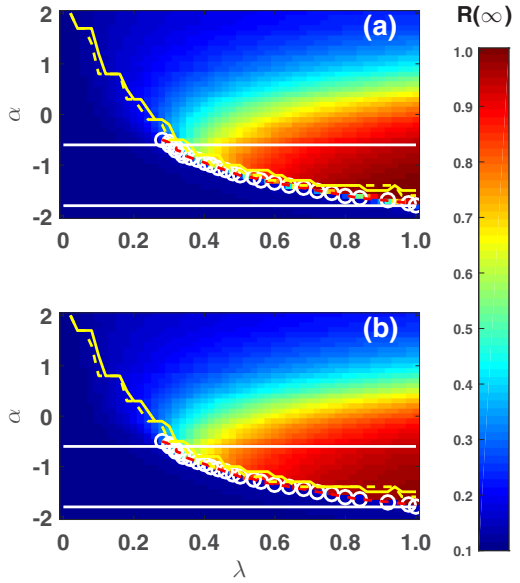

FIG. 4. Phase diagram of the final adoption size in the two-parameter (λ, α) space. (a) The color-coded values of $R(\infty)$ are from numerical simulations and (b) the color-coded values of $R(\infty)$ are from theoretical predictions. In all panels, the horizontal white lines indicate the critical preferential exponents $\alpha_c^d \approx -1.8$ and $\alpha_c^u \approx -0.6$, respectively. White circles and red dashed curve, respectively, represent the numerical and the theoretical λ_c values. The yellow solid curves and yellow dashed curves are numerical and the theoretical results of α_o. Other parameters are $\nu = 2.1$, $c = 4$, $\kappa = 3$, and $\gamma = 0.1$.

in the network. An appropriate value of $\alpha < 0$ (e.g., $\alpha_o \approx -1$ for $\lambda = 0.48$) can make a large number of small-degree nodes be contacted more frequently and easier to meet the threshold condition, which enhances the behavior spreading.

For the explosive growth, identifying its critical point is of great significance in prevention and control of complex contagions on networks. To determine the critical information transmission rate λ_c in simulations, we use the variability measure [35] as

$$\chi = \frac{\sqrt{(\langle R^2(\infty)\rangle - \langle R(\infty)\rangle^2)}}{\langle R(\infty)\rangle}, \tag{21}$$

where $\langle ...\rangle$ denotes the ensemble averaging of $R(\infty)$ and $\langle R(\infty)\rangle$ and $\langle R^2(\infty)\rangle$ are the first and second moments of $R(\infty)$, respectively. As a function of the effective infection rate λ, the variability measure reaches its maximum value at the critical point λ_c. Meanwhile, we determine the theoretical λ_c by calculating the jump size of $R(\lambda, \infty)$ versus λ curve obtained by the numerical iteration method. The jump size of final adoption size is defined as

$$\Delta R(\lambda, \infty) = R(\lambda, \infty) - R(\lambda - \Delta\lambda, \infty), \tag{22}$$

where $\Delta\lambda$ is the increment in λ and is set to be $\Delta\lambda = 0.005$. We can obtain the theoretical critical point λ_c when $\Delta R(\lambda, \infty)$ reaches its maximum value. When an explosive growth occurs, there is a large jump size of $R(\lambda, \infty)$ [i.e., a large $\Delta R(\lambda, \infty)$] at the critical point. Therefore, we assume that the peak value of jump size of final adoption size $\Delta R(\lambda, \infty)_{\max} \geqslant \epsilon$ indicates the existence of an explosive growth [36,37]. Without loss of generality, we set $\epsilon = 0.1$.

The numerical and theoretical critical points of social contagions are compared in Fig. 3. Figure 3(a) shows the final adoption size $R(\infty)$ grows explosively with the information transmission rate λ near $\lambda = 0.4$. From Fig. 3(b), it can be seen that the numerical critical point from Eq. (21) is $\lambda_c = 0.415$ and the theoretical critical point from Eq. (22) is also $\lambda_c = 0.415$. The theoretical results obtained by the dynamic message-passing method agree well with the simulation results.

We further determine how the preferential exponent α influences the complex contagion dynamics. Figure 4 shows the two-parameter (λ, α) phase diagram. The theoretical results in Fig. 4(b) are consistent with the simulation results in Fig. 4(a). From Figs. 4(a) and 4(b), we can see that the dependence of $R(\infty)$ on λ changes from being continuous to explosive and then to continuous with the increase of α. In particular, there are two critical preferential exponents α_c^d and α_c^u. When α is greater than α_c^d and smaller than α_c^u, $R(\infty)$ grows explosively with λ. When α is smaller than α_c^d or greater than α_c^u, the dependence of $R(\infty)$ on λ is continuous. In explosive growth regime with $\alpha \in (\alpha_c^d, \alpha_c^u)$, the critical information transmission rate λ_c decreases with the increase of preferential exponent α. When α is small, all the nodes in the network tend to contact the neighbors with small degrees in the contact process. In this case, more small-degree nodes can be contacted on average several times by the adopted nodes. To make these small-degree nodes meet the threshold condition, a greater information transmission rate λ_c should be required. Meanwhile, we see that the optimal preferential exponent α_o decreases with the increase of λ (see yellow solid

TABLE I. The structural characteristics of the two empirical networks, including the number of nodes N, the number of edges E, average degree $\langle k\rangle$, assortativity coefficient r, and clustering coefficient C.

	N	E	$\langle k\rangle$	r	C
Hamsterster friendships	1 858	12 534	13.492	−0.0846	0.00904
U. Rovira i Virgili	1 133	5 451	9.622	+0.0782	0.1662

and yellow dashed curves) and converges to the curve of λ_c versus α in the explosive growth regime (see white circles and red dashed curves). The convergence phenomenon means that these two results come from the the same reason (refer to the qualitative explanation of α_o versus λ before).

Finally, we verify the above results on empirical networks such as Hamsterster friendships network [38] and U. Rovira i Virgili network [39]. The structural characteristics of the two empirical networks are summarized in Table I. As shown in Fig. 5, both the crossover phenomenon of growth type and the optimal phenomenon of final behavior adoption size are found on the empirical networks. It is noted that there are some deviations between numerical results and theoretical predictions. From Refs. [27,40], we know that the dynamic message-passing method can not accurately capture the strong dynamical correlations among neighboring nodes caused by complex structural characteristics of the empirical networks. The dynamical correlation and network communicability are critically important to social contagion dynamics, for which an accurate theoretical framework is lacking, such as a higher-order mean-field framework. Another factor is the network size and the dynamic message-passing method is more accurate for networks with larger size (see Fig. 6 in Appendix A). Moreover, we investigate the effects of network size and mean degree on the behavior spreading, and similar results can be obtained (see Figs. 7 and 8 in Appendix B).

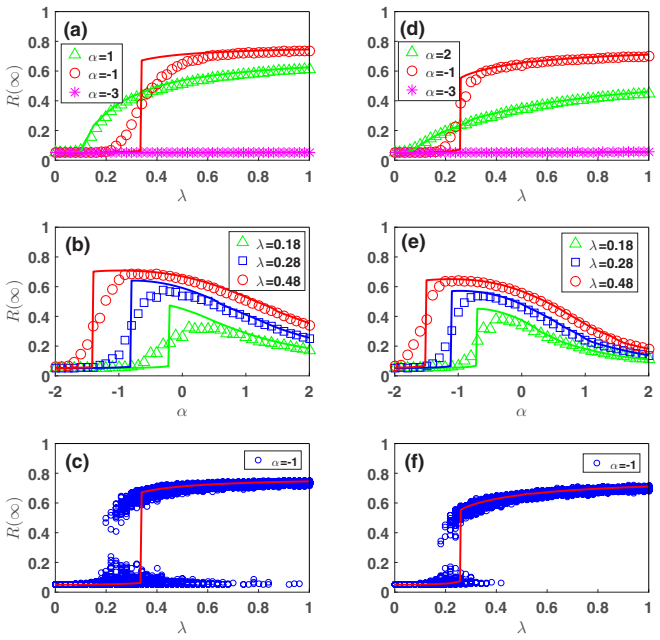

FIG. 5. Effects of preferential contacts on complex contagions on U. Rovira i Virgili network and Hamsterster friendships network. $R(\infty)$ as a function of λ for different values of α on U. Rovira i Virgili network (a) and Hamsterster friendships network (d), where green up triangles, red circles, and mauve asterisks represent the simulation results for $\alpha = 2.0, -1.0, -3.0$, respectively. $R(\infty)$ as a function of α for different λ values on U. Rovira i Virgili network (b) and Hamsterster friendships network (e), where red circles, blue squares, and green up triangles represent the simulation results for $\lambda = 0.48, 0.28, 0.18$, respectively. The explosive growth of the final adoption size $R(\infty)$ with the information transmission rate λ on U. Rovira i Virgili network (c) and Hamsterster friendships network (f), where each circle represents the result of one dynamical realization. In all panels, the curves are the theoretical predictions from Eqs. (2)–(4), (7), and (15). Other parameters are $c = 8, \kappa = 3, A_0 = 0.05$, and $\gamma = 0.1$.

V. DISCUSSION

The preferential contact process exists in nature and society widely, which has a significant impact on spreading dynamics. In this paper, we proposed a behavior spreading model based on the preferential contact process. A dynamic message-passing method was used to quantitatively understand the effects of the preferential contact process on the behavior spreading. The theoretical predictions from the suggested method agree well with the results from numerical simulations on strong heterogenous networks. We found that the preferential contact mechanism can lead to a crossover phenomenon between the two types of dependence: when α is a small negative value in the regime $\alpha \in (\alpha_c^d, \alpha_c^u)$, the final adoption size increases explosively with the information transmission rate; when α is smaller than α_c^d or greater than α_c^u, the final adoption size grows continuously with the information transmission rate. Moreover, the final adoption size $R(\infty)$ increases first and then decreases with the preferential exponent α. There is an extreme point (α_o, R_o) at a fixed λ. And the optimal preferential exponent α_o for complex contagions decreases as λ increases, which is obviously different from $\alpha_o = -1$ for simple contagions.

In this work, we studied how the preferential contact process influences the complex social contagions by using theoretical analyses and numerical simulations. We found that hub nodes with large degrees have a significant promotion effect on the spreading when the information transmission rate is small, while the nodes with small degrees play an important role in the behavior spreading when the information transmission rate is large. This work helps to deepen our understanding of social contagions in the preferential contact process. A strategy for controlling behavior spreading based on preferential contact may be an interesting and meaningful topic. However, there are some limitations in our model. For example, we consider that the preferential contact process depends on the node's degree. This mechanism is reasonable in the real society. In Sina Weibo, users tend to send messages to users with a large number of friends such as internet celebrity to gain more attention. Although our hypothesis is a reasonable extension, a more widely accepted fact is that the interaction mechanism between individuals is

very complicated. It is meaningful to consider the following questions: (a) What is the specific mechanism of preferential contacts between individuals in real social networks? (b) How does the preferential contacts between individuals affect the dynamics of social contagions, and is it inhibiting spreading or promoting spreading?

ACKNOWLEDGMENTS

This work was supported by the National Natural Science Foundation of China under Grants No. 11975099, No. 11575041, No. 11875132, No. 11872182, and No. 11835003, the Natural Science Foundation of Shanghai under Grants No. 18ZR1412200 and No. 18ZR1411800, and the Science and Technology Commission of Shanghai Municipality under Grant No. 14DZ2260800.

APPENDIX A: THE EFFECTS OF NETWORK SIZE ON THE ACCURACY OF DYNAMIC MESSAGE-PASSING METHOD

Here we investigate the effects of the network size N on the accuracy of the dynamic message-passing method. Figure 6 shows a comparison of theoretical predictions with simulation results on uncorrelated configuration networks with different network sizes. We can see that the dynamic message-passing method is more accurate for a larger value of N.

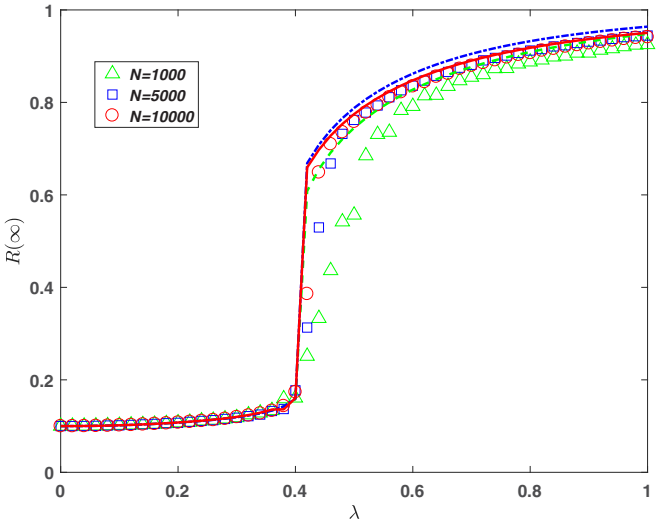

FIG. 6. Effects of network size on the accuracy of the dynamic message-passing method. $R(\infty)$ as a function of λ for different values of N, where the green up triangles, blue squares and red circle, respectively, represent the simulation results for $N = 1\,000, 5\,000, 10\,000$. And the green solid, blue dotted and red dot-dashed curves represent the theoretical predictions for $N = 1\,000, 5\,000, 10\,000$ from Eqs. (2)–(4), (7), and (15), respectively. Other parameters are $\nu = 2.1$, $c = 4$, $\kappa = 3$, $A_0 = 0.1$, and $\gamma = 0.1$.

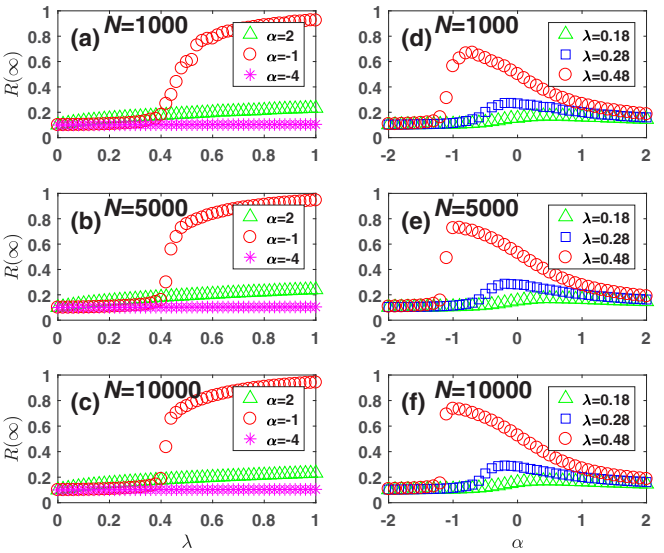

FIG. 7. Effects of network size on the behavior spreading. Other parameters are $\nu = 2.1$, $c = 4$, $\kappa = 3$, $A_0 = 0.1$, and $\gamma = 0.1$.

APPENDIX B: THE EFFECTS OF NETWORK SIZE AND MEAN DEGREE ON THE BEHAVIOR SPREADING IN THE PREFERENTIAL CONTACT PROCESS

We verify the main results on uncorrelated heterogeneous networks with different network sizes and mean degrees. As shown in Figs. 7 and 8, there is a crossover phenomenon of growth type on these networks. We also find that the final adoption size $R(\infty)$ first increases and then decreases with the increase of α. There exists an extreme point (α_o, R_o).

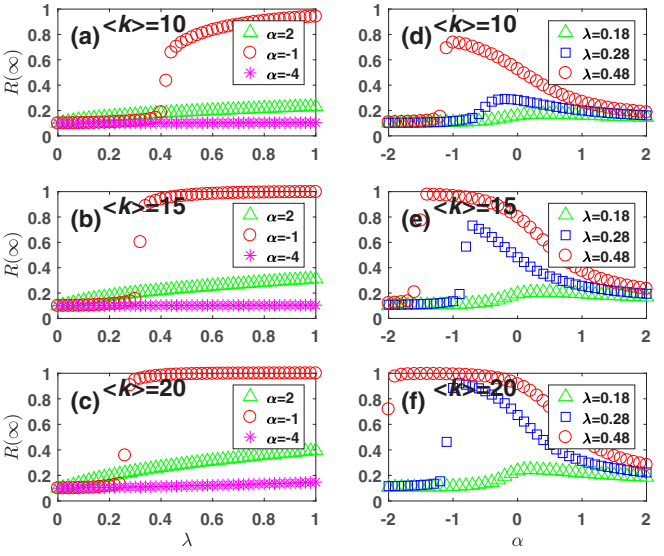

FIG. 8. Effects of mean degree on the behavior spreading. Other parameters are $\nu = 2.1$, $c = 4$, $\kappa = 3$, $A_0 = 0.1$, and $\gamma = 0.1$.

[1] P. Wang, M. C. González, C. A. Hidalgo, and A. L. Barabási, Science **324**, 1071 (2009).

[2] M. E. J. Newman, *Networks: An Introduction* (Oxford University Press, Oxford, UK, 2010).

[3] R. Pastor-Satorras and A. Vespignani, Phys. Rev. Lett. **86**, 3200 (2001).

[4] J. P. Gleeson and R. Durrett, Nat. Commun. **8**, 1227 (2017).

[5] R. Pastor-Satorras and A. Vespignani, Phys. Rev. E **63**, 066117 (2001).

[6] Y. Bai and Z. Jin, Chaos, Solitons Fractals **26**, 559 (2005).

[7] B. Wu, S. J. Mao, J. Z. Wang, and D. Zhou, Phys. Rev. E **94**, 062314 (2016).

[8] A. Banerjee, A. G. Chandrasekhar, E. Duflo, and M. O. Jackson, Science **341**, 1236498 (2013).

[9] L. Y. Lü, D. B. Chen, and T. Zhou, New J. Phys. **13**, 123005 (2011).

[10] P. S. Dodds and D. J. Watts, Phys. Rev. Lett. **92**, 218701 (2004).

[11] R. Pastor-Satorras, C. Castellano, P. Van Mieghem, and A. Vespignani, Rev. Mod. Phys **87**, 925 (2015).

[12] M. Zheng, L. Lü, M. Zhao *et al.*, Phys. Rev. E **88**, 012818 (2013).

[13] D. J. Watts, Proc. Nat. Acad. Sci. USA **99**, 5766 (2002).

[14] N. Perra, B. Gonçalves, R. Pastor-Satorras, and A. Vespignani, Sci. Rep. **2**, 469 (2012).

[15] J. Ugander, L. Backstrom, C. Marlow, and J. Kleinberg, Proc. Natl. Acad. Sci. USA **109**, 5962 (2012).

[16] C. Castellano and R. Pastor-Satorras, Phys. Rev. Lett. **96**, 038701 (2006).

[17] A.-X. Cui, W. Wang, M. Tang, Y. Fu, X.-M. Liang, and Y. Do, Chaos **24**, 033113 (2014).

[18] R. Yang, B.-H. Wang, J. Ren, W.-J. Bai, Z.-W. Shi, W.-X. Wang, and T. Zhou, Phys. Lett. A **364**, 189 (2007).

[19] W. Wang, P. Shu, Y.-X. Zhu, M. Tang, and Y.-C. Zhang, Chaos **25**, 103102 (2015).

[20] R. A. Hill and R. I. Dunbar, Hum. Nature **14**, 53 (2003).

[21] G. Miritello, E. Moro, R. Lara, R. Martínez-López, J. Belchamber, S. G. Roberts, and R. I. Dunbar, Soci. Netw. **35**, 89 (2013).

[22] R. Yang, T. Zhou, Y.-B. Xie, Y.-C. Lai, and B.-H. Wang, Phys. Rev. E **78**, 066109 (2008).

[23] L. Gao, W. Wang, L.-M. Pan, M. Tang, and H.-F. Zhang, Sci. Rep. **6**, 38220 (2016).

[24] W. Wang, M. Tang, H.-F. Zhang, and Y.-C. Lai, Phys. Rev. E **92**, 012820 (2015).

[25] B. Schönfisch and A. de Roos, BioSystems **51**, 123 (1999).

[26] H. Toyoizumi, S. Tani, N. Miyoshi, and Y. Okamoto, Phys. Rev. E **86**, 021103 (2012).

[27] M. Shrestha and C. Moore, Phys. Rev. E **89**, 022805 (2014).

[28] F. Krzakala, C. Moore, E. Mossel, J. Neeman, A. Sly, L. Zdeborová, and P. Zhang, Proc. Nat. Acad. Sci. USA **110**, 20935 (2013).

[29] M. Shrestha, S. V. Scarpino, and C. Moore, Phys. Rev. E **92**, 022821 (2015).

[30] L. A. Adamic and B. A. Huberman, Science **287**, 2115 (2000).

[31] B. Viswanath, A. Mislove, M. Cha, and K. P. Gummadi, in *Proceedings of the 2nd ACM Workshop on Online Social Networks* (ACM, New York, NY, 2009), pp. 37–42.

[32] M. Catanzaro, M. Boguná, and R. Pastor-Satorras, Phys. Rev. E **71**, 027103 (2005).

[33] M. Boguná, R. Pastor-Satorras, and A. Vespignani, Eur. Phys. J. B. **38**, 205 (2004).

[34] P. Shu, W. Wang, M. Tang, P. Zhao, and Y.-C. Zhang, Chaos **26**, 063108 (2016).

[35] P.-P. Shu, W. Wang, M. Tang, and Y. Do, Chaos **25**, 063104 (2015).

[36] J. Nagler, A. Levina, and M. Timme, Nat. Phys. **7**, 265 (2011).

[37] X.-L. Chen, R.-J. Wang, M. Tang, S.-M. Cai, H. E. Stanley, and L. A. Braunstein, New J. Phys. **20**, 013007 (2018).

[38] Hamsterster friendships network dataset—KONECT (2017), http://konect.cc/networks/petster-friendships-hamster/.

[39] U. Rovira i Virgili network dataset—KONECT (2017), http://konect.cc/networks/arenas-email.

[40] W. Wang, M. Tang, H. E. Stanley, and L. A. Braunstein, Rep. Prog. Phys. **80**, 036603 (2017).